PCCP

PAPER

View Article Online
View Journal | View Issue

Cite this: *Phys. Chem. Chem. Phys.*, 2017, **19**, 32235

Control of chemical chaos through medium viscosity in a batch ferroin-catalysed Belousov–Zhabotinsky reaction

Marcello A. Budroni, *[a] Ilaria Calabrese, [b] Ylenia Miele,[c] Mauro Rustici,[a] Nadia Marchettini [d] and Federico Rossi *[c]

Received 27th September 2017,
Accepted 16th November 2017

DOI: 10.1039/c7cp06601e

rsc.li/pccp

In this paper we show that the active interplay of nonlinear kinetics and transport phenomena in a chemical oscillator can be exploited to induce and control chaos. To this aim we use as a model system the ferroin-catalysed Belousov–Zhabotinsky (BZ) oscillating reaction, which is known to evolve to characteristic chaotic transient dynamics when carried out under batch and unstirred conditions. In particular, chemical chaos was found to appear and disappear by following a Ruelle–Takens–Newhouse (RTN) scenario. Here we use medium viscosity as a bifurcation parameter to tune the reaction–diffusion–convection (RDC) interplay and force the reaction in a specific sequence of dynamical regimes: either (i) periodic → quasi-periodic → chaotic or (ii) periodic → quasi-periodic or (iii) only periodic. The medium viscosity can be set by adding different amounts of surfactant (sodium dodecyl sulphate), known to have a little impact on the reaction mechanism, above its critical micelle concentration. Experimental results are supported by means of numerical simulations of a RDC model, which combines self-sustained oscillations to the related chemically-induced buoyancy convection.

1 Introduction

Deterministic chaos is one of the most striking manifestations of the intrinsic complex mechanisms ruling the evolution of nonlinear dynamical systems. The appearance of chaotic regimes can be sometimes desirable, for example, to enhance the mixing rate in a chemical reactor or as a means to encrypt binary messages and implement fundamental logic.[1,2] However, most often, chaos is a phenomenon that has to be avoided or at least controlled. Many theoretical and experimental models have been developed to study and fine tune the innermost mechanisms responsible for the onset of chaotic dynamics in physical, mechanical, biological and chemical systems.[3] In particular, the Belousov–Zhabotisky (BZ) reaction[4] is the most thoroughly studied chemical oscillator and still represents a paradigmatic model for understanding nonlinear dynamics in chemistry.[5] The BZ reaction is probably the simplest closed macroscopic system that can be maintained far-from-equilibrium by an internal source of free energy.[6] During the catalytic oxidation of an organic substrate (generally malonic acid) by an oxy-halogen species (for example BrO_3^-) in an acidic environment, oscillations in the intermediates and redox catalyst concentrations take place thanks to a complex nonlinear multi-step reaction mechanism.[7]

When performed in open reactors (CSTR), the temporal behaviour of the BZ reaction is mainly dictated by the flow rate of the reactants, and can switch from periodic at low rates to complex oscillatory patterns (quasi-periodic and eventually chaotic) for higher rates.[8–12]

In our previous studies,[13,14] we demonstrated that temporal and spatio-temporal chaos may also arise when the BZ reaction is carried out in batch unstirred reactors. Chaos can be detected both *via* potentiometric and spectrophotometric techniques and typically appears as a transient dynamical regime, between two periodic areas, by following a direct and inverse Ruelle–Takens–Newhouse (RTN) scenario,[15] both in cerium- and ferroin-catalysed BZ systems. The sensitivity to initial conditions, quite elusive in experimental systems, was isolated for these chaotic dynamics and also discussed as an educational example of this distinctive feature of chaos.[50] The cerium catalysed reaction has been thoroughly characterised under several experimental conditions[16–21] and the crucial role of the transport phenomena in the transition from periodic to aperiodic chemical oscillations has been assessed by means of theoretical models and numerical simulations.[22,23] Chaotic oscillations are the result of the active interplay of the oscillations of the BZ intermediates with the related chemically-driven convection.

[a] *Dipartimento di Chimica e Farmacia, Università di Sassari, Italy. E-mail: mabudroni@uniss.it*
[b] *Istituto Zooprofilattico Sperimentale della Sicilia, Area Chimica e Tecnologie Alimentari, Palermo, Italy*
[c] *Department of Chemistry and Biology "A. Zambelli", University of Salerno, Italy. E-mail: frossi@unisa.it*
[d] *Department of Earth, Environmental and Physical Sciences – DEEP Sciences, University of Siena, Italy*

In detail, reaction–diffusion processes, which are normally set in unstirred media, generate chemical patterns such as fronts and waves that feature local concentration heterogeneities spatially distributed through the reactive solution. If buoyancy- or/and surface-driven forces are at play, density and surface tension gradients associated with these chemical structures can trigger hydrodynamic flows that, in turn, couple with the spatio-temporal evolution of the reaction–diffusion structures. In general this active reaction–diffusion–convection (RDC) coupling, also called chemo-hydrodynamic coupling,[24] can rule the overall dynamics of such systems and sustain complex spatio-temporal patterns.[25–35] RDC dynamics can be governed and strongly depend on the experimental conditions of the system such as temperature, reactor size and reactant concentration, and on the changes that the chemical reaction is able to induce in the medium properties such as viscosity, density and surface tension. All these dependencies can be suitably included and described by pertinent dimensionless numbers (typically Grashof, Rayleigh and Marangoni numbers).[24]

Recently an externally forced RDC mechanism was also used to promote chaotic oscillations in a chemical system where a solution of photochromic spiro-oxazine irradiated with UV light only at the bottom of the reactor develops convective motions combined with changes (switch between *cis*- and *trans*-) in the configuration of spiro-oxazine. The resulting chaotic signals, recorded spectrophotometrically, were used to implement all the fundamental Boolean two-input-one-output logic gates.[2,36]

In this paper we show how the cooperative interplay of an oscillatory kinetics and buoyancy-driven hydrodynamic instabilities can be exploited as a general pathway to initiate, *in situ*, and control self-sustained chemical chaos. To this aim we use as a model system the ferroin catalysed BZ reaction and tune the solution viscosity, thus critically affecting the resistance of the reactive medium to hydrodynamic instabilities.

Experimentally, we introduce a sodium dodecyl sulphate (SDS) anionic surfactant in the BZ medium and vary its concentration above the critical micelle concentration (CMC) to increase the solution viscosity. SDS was found to slightly alter the kinetics of the BZ reaction, without changing the oscillation mechanism and without introducing new dynamical features,[37] conversely, for example, to the case of the zwitterionic surfactant *N*-tetradecyl-*N*,*N*-dimethylamine oxide that was found to cause an induction period prior to the onset of regular oscillations.[38–40] Therefore, the use of SDS impacts mainly the viscosity of the solution that, in turn, affects the onset of natural convection.

To support experimental scenarios we also develop a RDC model, where the kinetics of a chemical oscillator is coupled to fickian diffusion and convective terms, and we present related numerical simulations where the viscosity of the system is varied through the pertinent parameters.

2 Experimental

Malonic acid ($CH_2(COOH)_2$, MA), sodium bromate ($NaBrO_3$), sulfuric acid (H_2SO_4), ferroin ($Fe(phen)_3^{2+}$, Fe) and SDS were purchased from Sigma Aldrich. All reagents were of analytical quality and were used without further purification. Deionised water from reverse osmosis (Elga, model Option 3) was used to prepare all the solutions. Aqueous stock solutions of reagents were prepared, by weight, at the following concentrations: [MA] = 3.5 M, [$NaBrO_3$] = 1.2 M, [H_2SO_4] = 5.0 M, [Fe] = 25 mM, [SDS] = 0.7 M.

The kinetics of the BZ reaction has been studied at 25.0 °C, by keeping constant the concentration of all BZ reagents ([MA] = 0.74 M, [$NaBrO_3$] = 0.28 M, [H_2SO_4] = 0.35 M, [Fe] = 0.93 mM) in solutions with increasing concentration of surfactant, ($0 < [SDS] < 100$ mM).

The reaction dynamics was monitored by recording the absorption of ferriin, the oxidized form of ferroin, at λ_{max} = 630 nm (ε = 620 M^{-1} cm^{-1}) using a UV-vis spectrophotometer (Beckman DU-640 single ray) equipped with a water circulation cryo-thermostat (Haake D8). The solution for the kinetic runs was prepared in a 5 mL vial by adding the appropriate volumes of stock solutions, considering a final volume of 3.0 mL. The obtained solutions were stirred for twenty minutes using a magnetic stirrer, then, were transferred to quartz cuvettes and placed on the spectrophotometer for data acquisition. Each kinetic measurement has been repeated at least three times in order to check the reproducibility of the experimental results. The time series obtained in this way were subjected to statistical-mathematical analysis.

Surface tension measurements were performed in the presence of BZ reagents, excluding the catalyst, at concentrations used for kinetic experiments, in order to determine the Critical Micelle Concentration (CMC) of SDS under the experimental conditions. The measurements were made at a temperature of 25.0 °C by means of an Automatic-KSV Sigma tensiometer, using the Wilhelmy plate method.

The viscosity (η) measurements were performed, at a temperature of 25.0 °C, by means of an Ostwald viscometer on BZ-free catalyst solutions, at different concentrations of SDS. The densities (ρ) of the solutions were previously measured, under the same experimental conditions, by using a flow densimeter (model 03D Sodev inc.). The relative viscosity has been calculated with respect to the BZ solution without surfactant as reference, through the formula $\eta_{rel} = \frac{\eta}{\eta_0} = \frac{t}{t_0}\frac{\rho}{\rho_0}$, where t and t_0 are the elution time of the solution containing the surfactant and the reference solution, respectively; and ρ_0 and η_0 are the density and the viscosity of the surfactant-free BZ medium, respectively.

3 Results and discussion

Fig. 1(a) reports a typical spectrophotometric time series of a ferroin-catalyzed BZ reaction under batch unstirred conditions. The transient dynamical regime in the interval 300–2800 s has been demonstrated to be a genuine manifestation of a chaotic behaviour,[14] which appears and disappears between two periodic regions through a RTN-type scenario. To control the viscosity of the solution, thus influencing the hydrodynamic motions

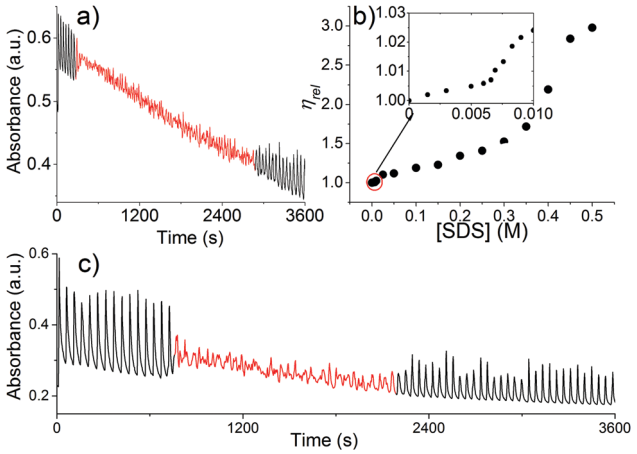

Fig. 1 (a) Ferroin-catalyzed BZ reaction in a batch unstirred reactor without SDS; red trace represents the chaotic transient between the two periodic regions (black trace). [MA] = 0.74 M, [$NaBrO_3$] = 0.28 M, [H_2SO_4] = 0.35 M, [Fe] = 0.93 mM, [SDS] = 0 M. (b) Relative viscosity of SDS solutions in the presence of [MA] = 0.74 M, [$NaBrO_3$] = 0.28 M, [H_2SO_4] = 0.35 M; the inset shows the zoom of the region 0 < [SDS] < 1×10^{-2} M. (c) Ferroin-catalyzed BZ reaction in a batch unstirred reactor in the presence of [SDS] = 1×10^{-2} M; red trace represents the chaotic transient between the two periodic regions (black trace). Reactant concentrations are the same as in (a).

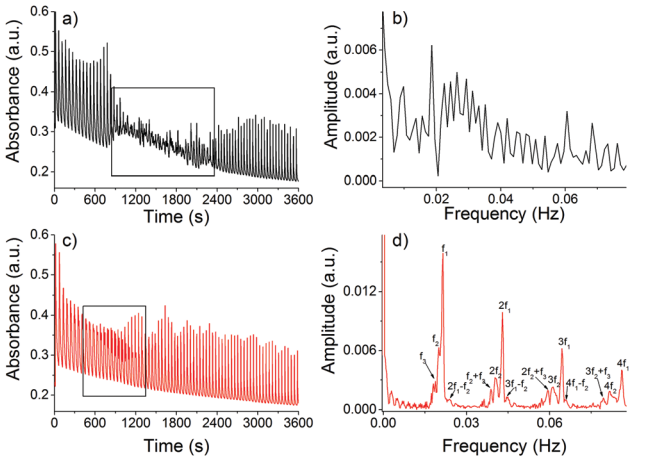

Fig. 2 Ferroin-catalyzed BZ reaction in a batch unstirred reactor in the presence of [SDS] = 1.15×10^{-2} M. [MA] = 0.74 M, [$NaBrO_3$] = 0.28 M, [H_2SO_4] = 0.35 M, [Fe] = 0.93 mM. (a) Chaotic dynamics as revealed by the broadband amplitude spectrum of the Fourier transform in (b). (c) Quasi-periodic dynamics with 3 fundamental frequencies whose ratio is an irrational number, as revealed by the Fourier transform in (d).

responsible for the onset of the chaotic regime, several experiments with increasing concentrations of surfactant were performed.

The critical micelle concentration of SDS under our experimental conditions was estimated as the intersection point of the two linear plots, above and below the CMC, of the surface tension *versus* log of surfactant concentration. CMC was estimated about 9.6×10^{-4} M at 25.0 °C in the presence of [MA] = 0.74 M, [$NaBrO_3$] = 0.28 M and [H_2SO_4] = 0.35 M. The lower value with respect to that in water ($\sim 8 \times 10^{-3}$ M) is in line with the effect caused by the presence of electrolytes.[41] The viscosity for the solutions with [SDS] > CMC was successively measured by means of the Ostwald method and the trend is reported in Fig. 1(b). η_{rel} starts to increase almost linearly with [SDS] above the CMC and has a sharp increase for [SDS] > 6×10^{-3} M, then, after a second linear region for 0.1 < [SDS] < 0.3 M, a second sharp increase is recorded for [SDS] > 0.3 M. Those jumps in the viscosity of the solutions are probably due to a change in the shape of the micelles and in the aggregation state of the surfactant.[37]

To maximise the effect of the surfactant on the viscosity of the solutions, we started to add SDS above the CMC. However we could not detect any difference in the reaction dynamics up to [SDS] = 1.15×10^{-2} M; below this threshold the transient chaotic regime is still present, though with a shorter lifetime. As an example Fig. 1(c) reports a time series where [SDS] = 1×10^{-2} M, corresponding to η_{rel} = 1.02, and the chaotic transient spans the interval 700–2200 s.

Fig. 2 shows the transition to a quasi-periodic regime when the concentration of the surfactant is increased to [SDS] = 1.15×10^{-2} M, corresponding to η_{rel} = 1.03. In the RTN scenario, the transition from a chaotic to a periodic regime takes place through the progressive disappearance of fundamental oscillation frequencies that brings the system from a strange attractor to a limit cycle in the phase space. Intermediate, or quasi-periodic, regimes are characterised by at least 2 fundamental oscillation frequencies (2D torus in the phase space); in principle nD tori (with $n \geq 3$) can be observed in the phase space, but they are generally unstable and tend to collapse into chaos. In this respect, the dynamics reported in Fig. 2 is a nice example of such behaviour and it is also a convincing demonstration of the dependence on the initial conditions of nonlinear systems. In fact, Fig. 2(a) and (c) show a BZ reaction performed under the same experimental conditions (reactant concentrations, temperature, preparation time, *etc.*) evolving into two different dynamical regimes, as shown by the Fourier transforms reported in panels (b) and (d). Panel (b) shows the broadband amplitude spectrum typical of chaos and relative to the framed region of the time series in panel (a); panel (d) shows the amplitude spectrum relative to the framed region in panel (c), where 3 fundamental frequencies (f_1 = 0.0215 Hz, f_2 = 0.0200 Hz and f_3 = 0.0188 Hz), whose ratio is an irrational number, and their linear combinations can be detected. In several experiments performed at η_{rel} = 1.03, the occurrence of the two behaviours was nearly 50%, confirming that the 3D torus is unstable and means that the system is close to the bifurcation point.

By further increasing the surfactant concentration, we could manage to complete the RTN scenario and bring the system to a periodic regime. Fig. 3 shows the time series for [SDS] = 1.25×10^{-2} M (η_{rel} = 1.04), where in the place of the chaotic transient and of the 3D torus is now present a 2D torus, as shown by the Fourier transform in panel (b); here 2 frequencies with an irrational ratio (f_1 = 0.361 Hz and f_2 = 0.0283 Hz) and their linear combinations can be assigned to all the peaks in the spectrum. Finally, for [SDS] = 2.5×10^{-2} M (η_{rel} = 1.10) the time series reported in panel (c) shows a periodic behaviour

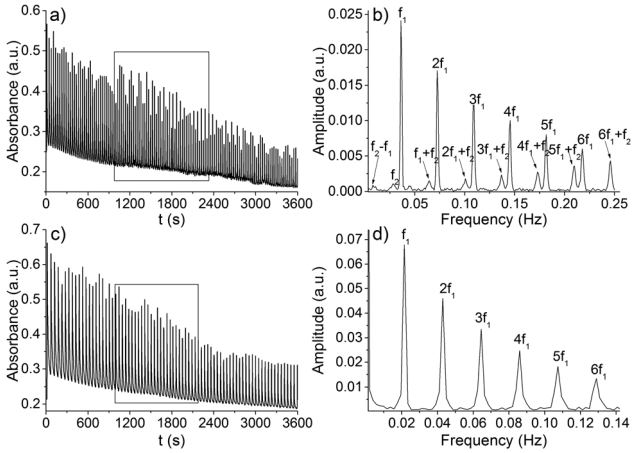

Fig. 3 Ferroin-catalyzed BZ reaction in a batch unstirred reactor in the presence of (a) [SDS] = 1.25×10^{-2} M showing a quasi-periodic dynamics with 2 fundamental frequencies as revealed by the Fourier transform in (b); and (c) [SDS] = 2.5×10^{-2} M showing a periodic dynamics with 1 fundamental frequency as revealed by the Fourier transform in (d). [MA] = 0.74 M, [$NaBrO_3$] = 0.28 M, [H_2SO_4] = 0.35 M, [Fe] = 0.93 mM.

with only one fundamental frequency (f_1 = 0.0215 Hz) as reported in panel (d). Both the 2D torus and the limit cycle are stable manifolds in the phase-space.

4 Numerical simulations

In order to assess viscosity as a convenient way to control the chemo-hydrodynamic coupling in the BZ medium and, hence, the transition through possible dynamical regimes, we investigate the BZ oscillations in a closed and unstirred reactor *via* a theoretical approach.

We model the system as a two-dimensional vertical slab (*i.e.* a vertical cut of the real three-dimensional spectrophotometric cuvette) in the coordinate system (x, z), with the gravitational field $\mathbf{g} = (0, -g)$ oriented against the vertical axis z. As shown in previous work, this two-dimensional description is a reliable approximation to the three-dimensional problem.[22,27,29,31] A set of reaction–diffusion–convection (RDC) equations is derived by coupling the chemical kinetics to diffusion through Fick's terms and to natural convection by means of the Navier–Stokes equations.

The presence of the surfactant SDS does not affect the oscillatory kinetics of the reaction which can be thus described by the well-known two-variable Oregonator model.[5,42] This model simplifies the highly complex kinetic scheme of the BZ, reducing the large number of species to two main chemical variables and preserving the essential features of the BZ dynamics. The related equations are derived in the pool chemical approximation, *i.e.* neglecting the consumption of the initial reactants as it occurs on a longer time scale than chemical oscillations, and quasi-stationary conditions are maintained for a long time even in batch reactors. The kinetic equations, written in the dimensionless form by using the Oregonator time scale, t_0,[23] are

$$\frac{dc_1}{dt} = \frac{1}{\varepsilon}\left[c_1(1-c_1) + fc_2\frac{q-c_1}{q+c_2}\right] = f_1(c_1, c_2, \bar{\kappa}), \quad (1)$$

$$\frac{dc_2}{dt} = c_1 - c_2 = f_2(c_1, c_2), \quad (2)$$

where c_1 and c_2 are the dimensionless concentrations of the autocatalytic intermediate species $HBrO_2$ and the oxidized catalyst, respectively, and $\bar{\kappa}$ is the set of kinetic parameters, $\bar{\kappa} = \{\varepsilon, q, f\}$. The initial distributions of the chemical species are set as

$$c_1(0) = 0.8 \quad \text{if } 0 < \theta < 0.5 \quad (3)$$

$$= c_{1(ss)} \quad \text{elsewhere} \quad (4)$$

$$c_2(0) = c_{2(ss)} + \frac{\theta}{8\pi f} \quad (5)$$

(where $c_{2(ss)} = c_{1(ss)} = q(f+1)/(f-1)$ and θ is the polar coordinate angle) to mimic inhomogeneous concentration profiles that typically occur in unstirred systems. These specific functions were used by Jahnke *et al.*[43] to initiate spiral waves in an analogous reaction–diffusion system. q and ε are kinetic parameters accounting for the excitability of the system and f is a stoichiometric factor included in the resetting step of the oscillatory scheme. This parameter allows one to set the system in an oscillatory regime when it ranges $[0.5,\ 1+\sqrt{2}]$ and we use f = 1.6; q is fixed arbitrarily to 0.01 instead that 0.0002 found by Tyson,[42] since increasing it up to a value 0.01 has little effect on rotating-wave solutions while speeding up numerical simulations;[43] ε = 0.01.

Hydrodynamic equations are derived in the Boussinesq approximation, *i.e.* assuming that density changes only affect the gravitational term, and the temperature terms are also neglected since it has been demonstrated that diffusion of chemicals is two orders of magnitude smaller than thermal diffusivity, thus representing the stronger source for the onset of convection.[44–46] The dimensionless form of the RDC system, written in the vorticity-stream function ($\omega - \psi$) form, reads (see details in ref. 31)

$$\frac{\partial c_i}{\partial t} + D_\nu\left(u\frac{\partial c_i}{\partial x} + v\frac{\partial c_i}{\partial z}\right) = D_i\nabla^2 c_i + f_i(c_j, \bar{\kappa})\ i, j = 1, 2, \quad (6)$$

$$\frac{\partial \omega}{\partial t} + D_\nu\left(u\frac{\partial \omega}{\partial x} + v\frac{\partial \omega}{\partial z}\right) = D_\nu\left(\nabla^2\omega - \sum_i \mathrm{Gr}_i\frac{\partial c_i}{\partial x}\right), \quad (7)$$

$$\frac{\partial^2\psi}{\partial x^2} + \frac{\partial^2\psi}{\partial z^2} = -\omega, \quad (8)$$

$$u = \frac{\partial\psi}{\partial z}, \quad (9)$$

$$v = -\frac{\partial\psi}{\partial x}. \quad (10)$$

The vorticity ω is defined as the curl of the dimensionless velocity field $(u,v)^T$ scaled over the velocity scale $v_0 = \nu/x_0$, where ν is the kinematic viscosity of the BZ medium and x_0 our length characteristic scale. $D_i = Dt_0/x_0^2$ = 0.00350 is the dimensionless diffusivity, with D being the dimensional diffusivities of the two species in the BZ medium assumed to be independent of the surfactant concentration.

The dimensionless parameters depending explicitly on viscosity are:

- $D_\nu = \nu t_0/{x_0}^2$, the dimensionless viscosity;
- The solutal Grashof number of the i-th species, Gr_i, defined as

$$\mathrm{Gr}_i = \frac{1}{\rho_0}\frac{\partial \rho}{\partial c_i}\frac{C_i^0 {x_0}^3 g}{\nu^2}. \quad (11)$$

Here g is the gravitational acceleration, $\frac{1}{\rho_0}\frac{\partial \rho}{\partial c_i}$ expresses the density variation due to concentration changes in the i-th intermediate with respect to the reference state ρ_0 characterizing the BZ medium and C_i^0 is the concentration scale of the i-th species.[5,23] Gr_i control the chemo-hydrodynamic coupling as they quantify the contribution of each chemical species to density-driven convective flows. Increasing the medium viscosity decreases Gr_i and, more concretely, the intensity of natural convection sustained by isothermal concentration gradients. Following relation (11), Gr_i is positive if the i-th species increases the local density of the medium and negative otherwise.

By writing the system viscosity as

$$\nu = \nu_0 \times \nu_{\mathrm{rel}}, \quad (12)$$

where ν_0 represents the kinematic viscosity of the aqueous BZ mixture, we can conveniently use ν_{rel} as a direct dimensionless parameter to control the system dynamics as in the experiments. This allows varying at once both D_ν and Gr_i.

The equation system (6)–(10) is solved by using the Alternating Direction Implicit Method (ADI)[47] over the dimensionless spatial domain of length $L_x = 50$ and height $L_z = 50$, discretized with a 100×100 point grid. Solutions were not substantially altered by increasing the spatial grid density.

We apply no-slip boundary conditions for the fluid velocity (*i.e.* $\psi = 0$)[48] and no-flux boundary conditions for the chemical concentration fields at the rigid walls of the slab. Due to the stiffness of the Oregonator model, simulations are run using a small integration time step $h_t = 1 \times 10^{-5}$, which ensures numerically stable and convergent solutions.

Experimental data (namely spectrophotometric time series) report as a function of time the solution absorbance (which is directly correlated to the catalyst concentration) averaged over the spatial domain scanned by the spectrophotometric beam. To compare numerical simulations with real experiments, we build the simulation time series by reporting at each time step the mean concentration of the oxidized catalyst, $\langle c_2(x,z,t)\rangle$, averaged over the solving grid. The dynamics reported hereunder corresponds to the transient regimes of the experiments where natural convection is fully set in, *i.e.* after stirring is stopped and, if possible, transitions to aperiodic behaviour should be visible. These regimes are framed in the experimental time series shown above. Differently from experiments, the signals obtained in the simulations are stationary because, as mentioned above, the reactants' depletion is neglected.

As a starting point of our parametric study, we consider the same value setting for which in our previous studies we obtained chaos in the same system:[22,23,27] $\mathrm{Gr}_1 = \mathrm{Gr}_2 = 12.1$, $D_\nu = 58.5$. The route from chemical chaos to regular periodic oscillations is then followed by increasing the relative viscosity of the medium, and, accordingly, reducing the starting value of Gr_i by a factor $1/{\nu_{\mathrm{rel}}}^2$, and increasing D_ν by ν_{rel}. In agreement with the experimental results, the system undergoes different dynamical regimes corresponding to a RTN scenario:

Chaotic regime

In Fig. 4a we show the typical aperiodic behaviour corresponding to $\nu_{\mathrm{rel}} = 1.00$. Similar dynamics are found in the range $\nu_{\mathrm{rel}} \in [1.00, 1.04]$. Within this parametric window the time series present high sensitivity to initial conditions and the signals diverge from each other if the initial concentrations of the chemical species are slightly varied. This is consistent with one of the most striking signatures of chaos. Also in Fig. 1(b), there is the amplitude FFT spectrum of the signal in panel (a). This shows a typical broadband, almost continuous, spectrum describing the infinite number of frequencies composing these chaotic oscillations, with a main contribution for small frequencies around 0.4. To further test and characterize chaos, we calculated in previous work[22] the largest Lyapunov exponent, λ, using the Rosestein algorithm from the TISEAN package[49] and we obtained $\lambda = 0.018$.

Quasi-periodic regime

As the relative viscosity ν_{rel} is increased to the value 1.05 a bifurcation to quasi-periodic behavior is found (see Fig. 5). The toroidal nature of the flow in the related phase space is confirmed by the Fourier amplitude spectrum in Fig. 5(b). Here we show the two fundamental frequencies $f_1 \sim 0.4, f_2 \sim 0.59$ characterising this regime, along with their main linear combinations and their harmonics. Note that the dominant contribution f_1 also present in the broadband spectrum of the chaotic regime is preserved. The ratio f_1/f_2 is an irrational number as expected for quasi-periodic oscillations.

Periodic regime

In Fig. 6 a numerical experiment carried out for $\nu_{\mathrm{rel}} = 1.24$ is shown. After a transient period (about 70 time units), the dynamics of the chemical species concentration switches to a regular periodic behaviour, here characterized by a limit cycle with one fundamental frequency $f_1 \sim 0.4$. Note that this frequency differs from that can be observed for the corresponding pure

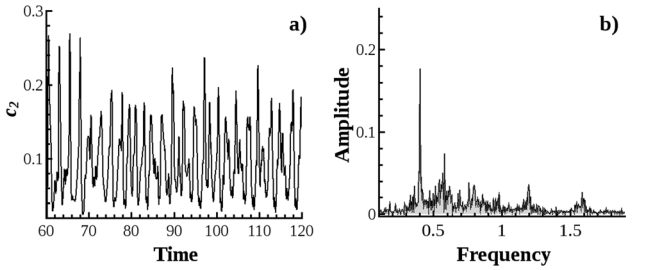

Fig. 4 Chaotic oscillations (a) and related amplitude Fourier spectrum (b) obtained for the RDC eqn (6)–(10) with $\nu_{\mathrm{rel}} = 1.00$.

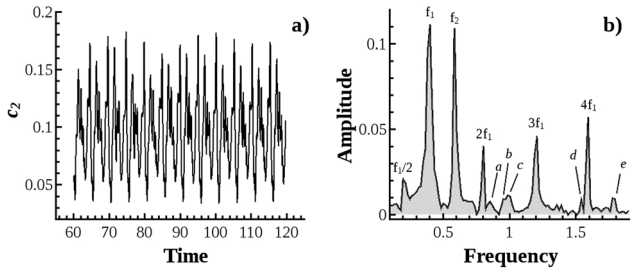

Fig. 5 Time series (a) and related amplitude Fourier spectrum (b) of the quasi-periodic regime obtained for the RDC eqn (6)–(10) with ν_{rel} = 1.10. $a = 9f_2 - 11f_2$, $b = 3f_2 - 2f_1$, $c = f_1 + f_2$, $d = 4f_2 + 2f_1$, $e = 3f_1 + f_2$.

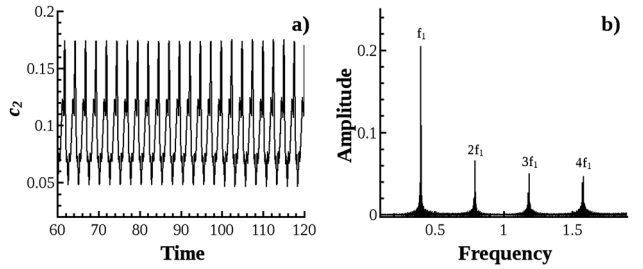

Fig. 6 Time series (a) and related amplitude Fast Fourier spectrum (b) of the periodic regime obtained from the RDC eqn (6)–(10) with ν_{rel} = 1.24.

reaction–diffusion system ($f_1 \sim 0.75$[22]), confirming the impact of the RDC interplay on the system dynamics. We observed that the frequency of the periodic oscillations increases to this limit as ν_{rel} is further increased beyond the threshold value of 1.23.

5 Conclusion

In summary, we investigated the RDC coupling in a chemical oscillator as a general method to induce and control *in situ* chaos. The transition from periodic to chaotic behaviours is chemically triggered by self-sustained oscillations that, coupled to diffusion, sustain pattern formation and, concretely, concentration heterogeneities. The related density gradients, if the action of the gravitational field is at play, start buoyancy-driven hydrodynamic flows that can feedback and complicate the spatio-temporal evolution of the reaction and even lead to chaos.

The RDC interplay can be suitably ruled both *via* kinetic and hydrodynamic parameters. Here we showed experimentally that by increasing the viscosity of the ferroin-catalyzed BZ medium through the introduction of a micellar SDS ionic surfactant, we can prevent the onset of the fingerprinting chaotic transient normally observed in the BZ carried out in aqueous solution.

Numerical simulations of the corresponding RDC model, where the Oregonator model is coupled to fickian diffusion and Navier–Stokes equations, agree with experimental results. They reveal a transition from a chaotic to a periodic regime by following a Ruelle–Takens–Newhouse scenario when the relative viscosity, affecting both the dimensionless viscosity and the Grashof numbers, is increased. Because of the batch conditions, an improved model should take into account the consumption of the reagents during the reaction evolution; however we already faced and modelled this feature in previous work.[23] Though we use some strong approximations in the system modelling, experimental features are not only qualitatively reproduced, but we can also find a semi-quantitative matching with simulations. In particular we observe that a comparable increment in the relative viscosity induces analogous effects on the system dynamics both in numerical and real experiments. This strengthens the general validity of the proposed chemo-hydrodynamic mechanism in chemical oscillators as a source for self-sustained chaos and a means to control it. This approach can be further exploited for implementing fundamental Boolean two-inputs-one-output logic as in previous studies[36] and for studying chaos synchronization in chemical systems.

Conflicts of interest

There are no conflicts to declare.

Acknowledgements

This paper is dedicated to the memory of Prof. Maria Liria Turco Liveri, in whose Lab part of these results was obtained. F. R. was supported by the grants ORSA158121 and ORSA167988 funded by the University of Salerno (FARB ex 60%). MAB and MR acknowledge financial support from the Fondazione Banco di Sardegna and Regione Sardegna.

References

1 S. Boccaletti, C. Grebogi, Y.-C. Lai, H. Mancini and D. Maza, *Phys. Rep.*, 2000, **329**, 103–197.
2 K. Hayashi, H. Gotoda and P. L. Gentili, *Chaos*, 2016, **26**, 053102.
3 E. Ott, C. Grebogi and J. A. Yorke, *Phys. Rev. Lett.*, 1990, **64**, 1196.
4 B. P. Belousov, *Sbornik Referatov po Radiatsonno Meditsine*, Moscow, 1958, pp. 145–147.
5 S. K. Scott, *Chemical Chaos*, Oxford University Press, Oxford, UK, 1993.
6 A. M. Zhabotinsky and F. Rossi, *Int. J. Ecodyn.*, 2006, **1**, 323–326.
7 A. F. Taylor, *Prog. React. Kinet. Mech.*, 2002, **27**, 247–325.
8 J. Wang, P. G. Soerensen and F. Hynne, *J. Phys. Chem.*, 1994, **98**, 725–727.
9 J. C. Wang, P. G. Sorensen and F. Hynne, *Z. Phys. Chem.*, 1995, **192**, 63–76.
10 B. R. Johnson, S. K. Scott and B. W. Thompson, *Chaos*, 1997, **7**, 350–358.
11 P. E. Strizhak and A. L. Kawczynski, *J. Phys. Chem.*, 1995, **99**, 10830–10833.
12 J. Wang, J. Zhao, Y. Chen, Q. Gao and Y. Wang, *J. Phys. Chem. A*, 2005, **109**, 1374–1381.
13 M. Rustici, C. Caravati, E. Petretto, M. Branca and N. Marchettini, *J. Phys. Chem. A*, 1999, **103**, 6564–6570.

14 F. Rossi, M. A. Budroni, N. Marchettini, L. Cutietta, M. Rustici and M. L. T. Liveri, *Chem. Phys. Lett.*, 2009, **480**, 322–326.
15 S. Newhouse, D. Ruelle and F. Takens, *Commun. Math. Phys.*, 1978, **64**, 35–40.
16 N. Marchettini and M. Rustici, *Chem. Phys. Lett.*, 2000, **317**, 647–651.
17 M. Rustici, R. Lombardo, M. Mangone, C. Sbriziolo, V. Zambrano and M. L. T. Liveri, *Faraday Discuss.*, 2002, **120**, 39–51.
18 M. Masia, N. Marchettini, V. Zambrano and M. Rustici, *Chem. Phys. Lett.*, 2001, **341**, 285–291.
19 M. L. T. Liveri, R. Lombardo, M. Masia, G. Calvaruso and M. Rustici, *J. Phys. Chem. A*, 2003, **107**, 4834–4837.
20 F. Rossi, F. Pulselli, E. Tiezzi, S. Bastianoni and M. Rustici, *Chem. Phys.*, 2005, **313**, 101–106.
21 L. Sciascia, F. Rossi, C. Sbriziolo, M. L. T. Liveri and R. Varsalona, *Phys. Chem. Chem. Phys.*, 2010, **12**, 11674–11682.
22 M. A. Budroni, M. Masia, M. Rustici, N. Marchettini, V. Volpert and P. C. Cresto, *J. Chem. Phys.*, 2008, **128**, 111102.
23 N. Marchettini, M. A. Budroni, F. Rossi, M. Masia, M. L. T. Liveri and M. Rustici, *Phys. Chem. Chem. Phys.*, 2010, **12**, 11062–11069.
24 A. D. Wit, K. Eckert and S. Kalliadasis, *Chaos*, 2012, **22**, 037101.
25 K. Matthiessen and S. C. Müller, *Phys. Rev. E: Stat., Nonlinear, Soft Matter Phys.*, 1995, **52**, 492–495.
26 M. Diewald, K. Matthiessen, S. C. Müller and H. R. Brand, *Phys. Rev. Lett.*, 1996, **77**, 4466–4469.
27 M. A. Budroni, M. Masia, M. Rustici, N. Marchettini and V. Volpert, *J. Chem. Phys.*, 2009, **130**, 024902.
28 L. Rongy and A. De Wit, *Phys. Rev. E: Stat., Nonlinear, Soft Matter Phys.*, 2008, **77**, 046310.
29 L. Rongy, G. Schuszter, Z. Sinko, T. Toth, D. Horvath, A. Toth and A. D. Wit, *Chaos*, 2009, **19**, 023110.
30 F. Rossi, M. A. Budroni, N. Marchettini and J. Carballido-Landeira, *Chaos*, 2012, **22**, 037109.
31 M. A. Budroni, L. Rongy and A. De Wit, *Phys. Chem. Chem. Phys.*, 2012, **14**, 14619–14629.
32 I. Berenstein and C. Beta, *J. Chem. Phys.*, 2012, **136**, 034903.
33 D. M. Escala, M. A. Budroni, J. Carballido-Landeira, A. De Wit and A. P. Muñuzuri, *J. Phys. Lett.*, 2014, **5**, 413–418.
34 R. Tiani, A. D. Wit and L. Rongy, *Adv. Colloid Interface Sci.*, 2017, DOI: 10.1016/j.cis.2017.07.020.
35 M. A. Budroni and A. De Wit, *Chaos*, 2017, **27**, 104617.
36 P. L. Gentili, M. S. Giubila and B. M. Heron, *ChemPhysChem*, 2017, **18**, 1831–1841.
37 F. Rossi, R. Lombardo, L. Sciascia, C. Sbriziolo and M. L. T. Liveri, *J. Phys. Chem. B*, 2008, **112**, 7244–7250.
38 F. Rossi, R. Varsalona and M. L. T. Liveri, *Chem. Phys. Lett.*, 2008, **463**, 378–382.
39 F. Rossi, R. Varsalona, N. Marchettini and M. L. Turco Liveri, *Soft Matter*, 2011, **7**, 9498.
40 M. A. Budroni and F. Rossi, *J. Phys. Chem. C*, 2015, **119**, 9411–9417.
41 E. Dutkiewicz and A. Jakubowska, *Colloid Polym. Sci.*, 2002, **280**, 1009–1014.
42 R. J. Field and M. Burger, *Oscillations and Travelling Waves in Chemical Systems*, Wiley, New York, USA, 1985.
43 W. Jahnke, W. E. Skaggs and A. T. Winfree, *J. Phys. Chem.*, 1989, **93**, 740–749.
44 Y. Wu, D. A. Vasquez, B. F. Edwards and J. W. Wilder, *Phys. Rev. E: Stat., Nonlinear, Soft Matter Phys.*, 1995, **51**, 1119–1127.
45 K. A. Cliffe, S. J. Tavener and H. Wilke, *Phys. Fluids*, 1998, **10**, 730–741.
46 C. Almarcha, P. M. J. Trevelyan, P. Grosfils and A. De Wit, *Phys. Rev. E: Stat., Nonlinear, Soft Matter Phys.*, 2013, **88**, 033009.
47 D. W. Peaceman and H. H. Rachford, *J. Soc. Ind. Appl. Math.*, 1955, **3**, 28.
48 L. Lemaigre, M. A. Budroni, L. A. Riolfo, P. Grosfils and A. De Wit, *Phys. Fluids*, 2013, **25**, 014103.
49 R. Hegger, H. Kantz and T. Schreiber, *Chaos*, 1999, **9**, 413.
50 M. A. Budroni, F. Wodlei and M. Rustici, *Eur. J. Phys.*, 2014, **35**, 045005.